

# The Mitochondrial-Derived Peptide Humanin Protects RPE Cells From Oxidative Stress, Senescence, and Mitochondrial Dysfunction

Parameswaran G. Sreekumar,<sup>1</sup> Keijiro Ishikawa,<sup>1</sup> Chris Spee,<sup>2</sup> Hemal H. Mehta,<sup>3</sup> Junxiang Wan,<sup>3</sup> Kelvin Yen,<sup>3</sup> Pinchas Cohen,<sup>3</sup> Ram Kannan,<sup>1</sup> and David R. Hinton<sup>2,4</sup>

<sup>1</sup>Arnold and Mabel Beckman Macular Research Center, Doheny Eye Institute, Los Angeles, California, United States

<sup>2</sup>Department of Ophthalmology, University of Southern California, Los Angeles, California, United States

<sup>3</sup>USC Leonard Davis School of Gerontology, University of Southern California, Los Angeles, California, United States

<sup>4</sup>Department of Pathology, University of Southern California, Los Angeles, California, United States

Correspondence: David R. Hinton, Department of Pathology, Keck School of Medicine, University of Southern California, 2011 Zonal Avenue, HMR 209, Los Angeles, CA 90089, USA; dhinton@usc.edu.

RK and DRH are joint senior authors.

Submitted: April 8, 2015

Accepted: February 8, 2016

Citation: Sreekumar PG, Ishikawa K, Spee C, et al. The mitochondrial-derived peptide humanin protects RPE cells from oxidative stress, senescence, and mitochondrial dysfunction. *Invest Ophthalmol Vis Sci*. 2016;57:1238-1253. DOI:10.1167/iov.15-17053

**PURPOSE.** To investigate the expression of humanin (HN) in human retinal pigment epithelial (hRPE) cells and its effect on oxidative stress-induced cell death, mitochondrial bioenergetics, and senescence.

**METHODS.** Humanin localization in RPE cells and polarized RPE monolayers was assessed by confocal microscopy. Human RPE cells were treated with 150  $\mu$ M tert-Butyl hydroperoxide (tBH) in the absence/presence of HN (0.5–10  $\mu$ g/mL) for 24 hours. Mitochondrial respiration was measured by XF96 analyzer. Retinal pigment epithelial cell death and caspase-3 activation, mitochondrial biogenesis and senescence were analyzed by TUNEL, immunoblot analysis, mitochondrial DNA copy number, SA- $\beta$ -Gal staining, and p16<sup>INK4a</sup> expression and HN levels by ELISA. Oxidative stress-induced changes in transepithelial resistance were studied in RPE monolayers with and without HN cotreatment.

**RESULTS.** A prominent localization of HN was found in the cytoplasmic and mitochondrial compartments of hRPE. Humanin cotreatment inhibited tBH-induced reactive oxygen species formation and significantly restored mitochondrial bioenergetics in hRPE cells. Exogenous HN was taken up by RPE and colocalized with mitochondria. The oxidative stress-induced decrease in mitochondrial bioenergetics was prevented by HN cotreatment. Humanin treatment increased mitochondrial DNA copy number and upregulated mitochondrial transcription factor A, a key biogenesis regulator protein. Humanin protected RPE cells from oxidative stress-induced cell death by STAT3 phosphorylation and inhibiting caspase-3 activation. Humanin treatment inhibited oxidant-induced senescence. Polarized RPE demonstrated elevated cellular HN and increased resistance to cell death.

**CONCLUSIONS.** Humanin protected RPE cells against oxidative stress-induced cell death and restored mitochondrial function. Our data suggest a potential role for HN therapy in the prevention of retinal degeneration, including AMD.

**Keywords:** humanin, senescence, cell death, cellular respiration, transepithelial resistance, receptors

Age-related macular degeneration (AMD) is the leading cause of severe and irreversible central vision loss among elderly populations worldwide. The primary site of AMD pathology is the retinal pigment epithelium (RPE),<sup>1,2</sup> a quiescent monolayer strategically located between the choriocapillaris/Bruch's membrane complex and the photoreceptors. Loss of normal physiological function in the aging RPE cells could result in the formation of drusen deposits seen in AMD retina. Large macular drusen and greater drusen area increase the risk of progression to the blinding late form of AMD.<sup>3</sup> One salient feature of late-stage "dry" AMD is the appearance of geographic atrophy, characterized by RPE cell loss, subsequent degeneration of photoreceptors, and thinning of retina.<sup>4</sup> Oxidative stress and oxidative stress-induced cellular senescence are known to contribute to the development of AMD.<sup>5-8</sup>

Humanin (HN) is a 21- to 24-amino-acid peptide expressed from an open reading frame within the mitochondrial 16S ribosomal RNA.<sup>9-13</sup> Alternatively, HN could also be encoded within one or more of the nuclear regions with 92% to 95% similarity to the original HN cDNA, dispersed in multiple copies throughout the human genome.<sup>9,14</sup> A recent study<sup>15</sup> demonstrated that in rat, HN homologue (Rattin; rHN) is derived from the mitochondrial genome and is translated in mitochondria. However, in human, it is still unclear whether HN is translated in the mitochondria (21-amino-acid peptide) or the cytoplasm (24-amino-acid peptide).<sup>13</sup> Humanin has cytoprotective, metabolic, and anti-inflammatory effects in multiple cell types and animal models, including beneficial effects of HN on H<sub>2</sub>O<sub>2</sub>-induced cell death,<sup>16</sup> amyloid A $\beta$  toxicity,<sup>9</sup> serum starvation-induced death of neuronal cells,<sup>17</sup> and oxidized LDL-induced death of vascular endothelial cells.<sup>18</sup> Humanin is expressed in a

TABLE. List of Antibodies

Target	Type	Source	Application	Vendor
Humanin	Polyclonal	Rabbit	IF, WB	In-house
CNTFR $\alpha$	Polyclonal	Goat	IF	Santa Cruz Biotechnology, CA, USA
gp130	Polyclonal	Rabbit	IF	Santa Cruz Biotechnology, CA, USA
WSX1	Polyclonal	Rabbit	IF	Sigma-Aldrich Corp., MO, USA
Cleaved caspase-3	Polyclonal	Rabbit	IF, WB	Cell Signaling Technology, MA, USA
p16 <sup>INK4a</sup>	Monoclonal	Rabbit	WB	Abcam, MA, USA
Phospho-STAT3 (Tyr 705)	Monoclonal	Rabbit	WB	Cell Signaling Technology, MA, USA
STAT3	Monoclonal	Rabbit	WB	Cell Signaling Technology, MA, USA
ZO1	Polyclonal	Rabbit	IF	Life Technologies, CA, USA
mtTFA	Monoclonal	Mouse	WB	Santa Cruz Biotechnology, CA, USA
GAPDH	Monoclonal	Mouse	WB	EMD Millipore, MA, USA

GAPDH, Glyceraldehyde-3-Phosphate Dehydrogenase; IF, immunofluorescence; WB, western blot.

variety of tissues, including neuronal cells,<sup>9,19</sup> skeletal muscles,<sup>20</sup> blood-derived cells,<sup>21</sup> and is also detected in plasma.<sup>22</sup> To our knowledge, no information is available on the expression and function of HN in the retina and RPE cells.

Several binding partners of HN have been identified; some of these are considered HN receptors.<sup>11,23</sup> Humanin mediates its neuroprotection through different pathways by binding to its specific receptor or target proteins. Humanin exerts its action by interfering with the proapoptotic factor Bax and with insulin-like growth factor (IGF)-binding protein 3 (IGFBP3) and by inhibiting signal transducer and activator of transcription 3 (STAT3).<sup>14,24</sup> Among the three putative HN receptors reported, the neuroprotective effect of HN occurs through a cell-surface receptor that belongs to the interleukin-6 receptor family.<sup>25,26</sup> This heterotrimeric HN receptor (htHNR) is derived from ciliary neurotrophic factor receptor  $\alpha$  (CNTFR $\alpha$ ), WSX-1, and gp130. The binding of HN to htHNR results in oligomerization of the receptor subunits and subsequent activation of JAK2 and STAT3.<sup>25-28</sup> Humanin-mediated neuroprotection could involve the activation of STAT3, which plays important roles in normal cellular responses to cytokines and growth factors.<sup>28</sup> In addition, HN binds to Bax, BimEL, or tBid and prevents translocation from cytoplasm to mitochondria, thereby protecting cells from apoptosis-inducing insults that trigger the mitochondrial pathway for cell death.<sup>14,29,30</sup>

Most of the neuroprotective studies on HN have been performed on neuronal cells and Alzheimer (AD)-related models. Because of suggested commonalities in the pathogenesis of AD and AMD,<sup>31</sup> and since very little is known about the role of HN in AMD, we investigated the role of HN in oxidative stress, a process linked to senescence and AMD. This study tested the hypothesis that exogenous administration of HN could inhibit oxidative stress-induced cell death in RPE cultures and polarized monolayers, in part by improving mitochondrial function and biogenesis. A possible role for HN in delaying RPE senescence was also studied.

## METHODS

### Retinal Pigment Epithelial Cell Culture

All procedures adhered to the tenets of the Declaration of Helsinki for research involving human subjects and were performed with the approval of the institutional review board of the University of Southern California under protocol No. HS-947005. The RPE cells were isolated from human fetal eyes obtained from Advanced Bioscience Resources Inc. (Alameda, CA, USA) and Novogenix Laboratories, LLC (Los Angeles, CA, USA) and cultured as previously described.<sup>32-34</sup> Confluent cell cultures from passages 2 to 4 were used. Highly differentiated

fetal human RPE cells were cultured on Transwell filters as described earlier.<sup>33</sup> Briefly, primary culture of human fetal RPE cells was trypsinized and resuspended in media supplemented with 10% fetal bovine serum (FBS). Approximately  $1.0 \times 10^5$  RPE cells/cm<sup>2</sup> were seeded on fibronectin-coated Transwell filters (12-mm internal diameter, 0.4- $\mu$ m pore size, Corning Inc, Corning, NY, USA). The RPE cells were cultured on the Transwell filters in 10% FBS containing medium for 1 day and in 1% FBS thereafter for 4 weeks. All polarized RPE monolayers expressed tight junction markers such as ZO1, occludin, and apical Na/K-ATPase and developed apical microvilli.<sup>33</sup> Polarized cultures were used once they obtained a transepithelial resistance (TER) greater than 300  $\Omega$ ·cm<sup>2</sup>.

### Localization of HN in RPE Cells

Source and other details of all antibodies are summarized in the Table. Localization of HN and its receptors was performed on just confluent RPE cells grown in four-well chamber slides and differentiated cells grown on permeable filters. After fixation with 4% paraformaldehyde (PFA) for 20 minutes, samples were blocked in 5% normal goat serum containing 0.1% Triton X-100 for 1 hour. Cells were incubated overnight with 1:100 dilution of HN, CNTFR $\alpha$ , WSX1, gp130 and for 30 minutes with FITC-labeled secondary antibodies. Samples were viewed under a laser scanning confocal microscope. In separate studies, RPE cells were incubated with Mitotracker Red CMXRos (500 nM; Life Technologies, Carlsbad, CA, USA) for 15 minutes before fixation and processing for HN staining.

### Protection of RPE Cells From Oxidative Stress

Just confluent RPE cells grown in four-well chamber slides were coincubated with varying doses (0.5–10  $\mu$ g/mL) of HN (custom synthesized, purity > 98%; NeoPeptide, Cambridge, MA, USA) and 150  $\mu$ M tert-Butyl hydroperoxide (tBH; Sigma-Aldrich Corp., St. Louis, MO, USA) or 150  $\mu$ M tBH alone for 24 hours in serum-free culture medium. For STAT3 inhibitor experiments (STAT3 inhibitor VII; Calbiochem, San Diego, CA, USA) just confluent cells were treated for 24 hours with 0.5  $\mu$ M inhibitor alone or with 10  $\mu$ g HN, 150  $\mu$ M tBH, and 0.50  $\mu$ M inhibitor. Cell death was studied by TUNEL staining (In Situ Cell Death Detection Kit; Roche Applied Science, Indianapolis, IN, USA). The TUNEL-positive cells were counted and quantified as previously described.<sup>35</sup> Cells were also stained for active caspase-3.<sup>35</sup> We also examined senescence markers to see whether our experimental conditions induced RPE senescence (see below for a detailed protocol).

### Uptake of FITC-Labeled HN Peptide by Human RPE Cells and Colocalization With Mitochondria

Fluorescein (FITC)-labeled HN (C-terminal) peptide was custom synthesized (NeoPeptide). Serum-starved just confluent RPE cells were incubated with 10  $\mu$ g FITC-labeled HN for 2 hours. Fifteen minutes before the cessation of the HN treatment, cells were incubated with 500 nM MitoTracker Red. Subsequently, cells were washed with PBS and fixed with 4% PFA for 10 minutes at room temperature. Uptake of labeled HN by RPE cells was examined under a spinning disc confocal microscope (PerkinElmer, Waltham, MA, USA).

### Detection of Mitochondrial Superoxide With MitoSOX

The production of superoxide in mitochondria was visualized with MitoSOX (Life Technologies). Just confluent RPE cells grown on four-well chamber slides were treated with 150  $\mu$ M tBH or 10  $\mu$ g HN or 10  $\mu$ g HN + 150  $\mu$ M tBH for 24 hours. Before termination of treatment, cells were incubated with 5  $\mu$ M MitoSOX for 15 minutes at 37°C. Cells were washed in PBS, fixed with 3.7% PFA for 15 minutes, washed, mounted with 4',6-diamidino-2-phenylindole (DAPI; Vector Laboratories, Burlingame, CA, USA), and viewed under a laser confocal microscope (LSM 510; Zeiss, Thornwood, NY, USA).

### Immunoblot Analysis

At the end of each experiment, protein was extracted from RPE cells and immunoblot analysis for active caspase-3, mitochondrial transcription factor A (mtTFA), and p16<sup>INK4a</sup> was performed.

### Quantification of HN Levels in Cell Lysates and RPE-Conditioned Medium by ELISA

Humanin levels of plasma and tissue extracts were measured by in-house HN ELISA developed by one of the authors (PC).<sup>22</sup> Rabbit antihuman polyclonal antiserum was raised against the human analogue HNG (which recognizes endogenous HN and yields a single band in Western blot in human RPE cultures). The IgG subclasses were purified by protein A column chromatography (Pierce Chemical Co, Rockford, IL, USA) and were used as the capture antibody. Immunoglobulin G was further purified with an HNG-conjugated ligand affinity column and labeled with biotin. This biotinylated ligand affinity-purified anti-HNG IgG was used as the detection antibody. To measure endogenous HN levels, synthetic HN purchased from Bachem (Torrance, CA, USA) was used as a standard within the range of 0.1 to 50 ng/mL. The intra- and interassay coefficient variations were less than 10%. Total cellular protein was extracted from just confluent and polarized RPE monolayers. Before performing the HN immunoassay, 200  $\mu$ g total protein in 100  $\mu$ L RIPA buffer (Thermo Scientific, Waltham, MA, USA) was extracted with acetonitrile/HCl solution. The supernatants were dried down by SpeedVac and the pellet was reconstituted with phosphate-buffered saline and 0.5% Tween 20. After centrifugation, the supernatants were used to measure HN by in-house ELISA, and HN levels were reported as pg/mg protein. The HN level in the conditioned media of just confluent nonpolarized RPE cells and polarized RPE monolayers (apical and basal media were collected and analyzed separately) grown in serum-free media for 24 hours was also analyzed by using the same method. Briefly, 200  $\mu$ L extraction reagent was added to 100  $\mu$ L conditional media,

gently mixed, and incubated at room temperature for 30 minutes. The mixture was centrifuged, the supernatant dried and reconstituted with 250  $\mu$ L phosphate buffer. Absorbance was measured on a plate spectrophotometer (Molecular Designs, Sunnyvale, CA, USA) at 490 nm.

### Measurement of Cellular Respiration

Cellular bioenergetics were determined by measuring oxygen consumption rate (OCR) of the cells with an XF-96 Flux Analyzer (Seahorse Biosciences, North Billerica, MA, USA). The RPE cells were seeded in XF 96-well cell culture microplates (Seahorse Bioscience). Just confluent RPE cells were treated for 24 hours with either 150  $\mu$ M tBH or 10  $\mu$ g HN, or a combination of both tBH and HN (5 or 10  $\mu$ g/mL). Assays were initiated by replacing the growth medium with 175  $\mu$ L XF assay medium (specially formulated, unbuffered Dulbecco's modified Eagle's medium for XF assays; Seahorse Bioscience) supplemented with 2 mM sodium pyruvate and 25 mM glucose, pH 7.4. The cells were kept in a non-CO<sub>2</sub>-incubator for 60 minutes at 37°C before placement in the Analyzer. The concentrations used for bioenergetic assessment were 1.0  $\mu$ M/mL for oligomycin (to inhibit ATP synthase activity), 2.4  $\mu$ M for tri-fluorocarbonylcyanide phenylhydrazone (FCCP) (to uncouple mitochondrial oxidative phosphorylation), and 1  $\mu$ M for rotenone and antimycin A (to inhibit electron transport in complex I and III). These mitochondrial inhibitors were used to determine a number of bioenergetic and mitochondrial function parameters, including basal respiration, ATP turnover rate, proton leak, and maximal and spare respiratory capacity.<sup>36,37</sup> In brief, the ATP-linked respiration was obtained from the difference between basal OCR and respiration after oligomycin injection. The difference between antimycin A and oligomycin respiration yielded proton leak. Maximal OCR was the difference in OCR between FCCP-induced respiration and OCR after the injection of antimycin A. Mitochondrial reserve capacity was the difference between maximal respiration and basal OCR. Each sample was measured in three to five wells per condition and the results were averaged. The experiments were repeated three or four times and the mean values averaged so that  $n = 3$  to 4 per condition.

### DNA Extraction and Mitochondrial DNA (mtDNA) Copy Number Measurement

DNA from just confluent RPE cells was extracted with a commercial kit (Qiagen, Valencia, CA, USA) and quantified (NanoDrop; Thermo Scientific, Wilmington, DE, USA). Mitochondrial copy number was estimated by real-time PCR (Light cycler 480; Roche) using two mtDNA targets (ND1, ND5) and two nuclear DNA targets (SLCO2B1, SERPINA1) (Clontech, Mountain View, CA, USA). The Q-PCR was performed in 20  $\mu$ L reaction mixture containing 10  $\mu$ L SYBR Green, 1  $\mu$ M of each primer, and DNA. The PCR reactions were subjected to hot start at 95°C for 5 minutes followed by 40 cycles of denaturation at 95°C for 5 seconds, annealing at 55°C for 5 seconds, and extension at 72°C for 20 seconds. The ratio of mtDNA to nuclear DNA was calculated by averaging the copy numbers of ND1/SLCO2B1 and ND5/SERPINA1.

### Counting Mitochondria by Transmission Electron Microscopy (TEM)

Transmission electron microscopy was used to count number of mitochondria. In brief, just confluent RPE cells after respective treatments were fixed in half-strength

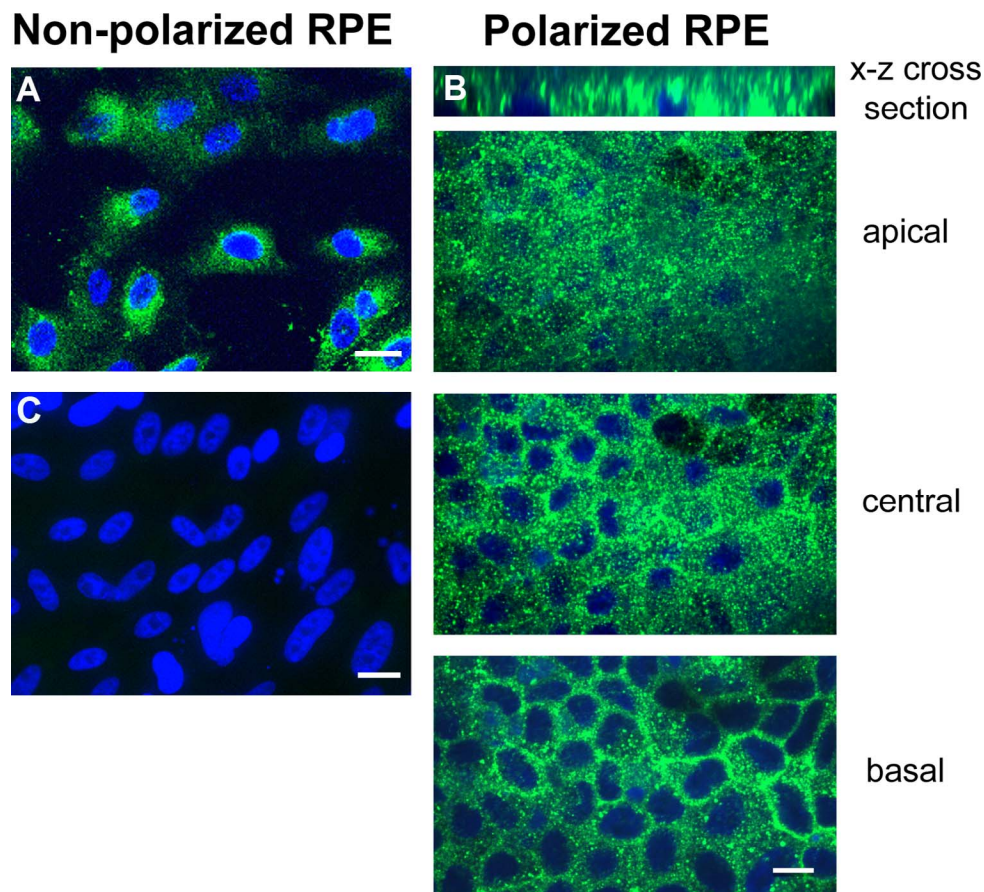


**FIGURE 1.** Localization of HN in RPE cells. Immunofluorescence staining of HN in nonpolarized RPE cells (A) and polarized RPE monolayer (B). Confocal images were taken at apical, central, and basal levels of the polarized RPE monolayer. Humanin (green) was localized both in the apical and basal domains as confirmed by the x-z cross-section stack image shown as the *top panel*. DAPI nuclear counterstain (blue). (C) “No primary antibody” control. Scale bar: 20  $\mu\text{m}$ .

Karnovsky's fixative, sectioned, and the grids were viewed under a digital electron microscope (JEOL-2100; JEOL, Peabody, MA, USA) at 80 KV. Mitochondria present per cell were counted and a total of 10 to 15 cells were examined in 4 to 5 different sections.<sup>38</sup> Data are presented as average number of mitochondria present per cell (mean  $\pm$  SEM).

### Analysis of Oxidative Stress–Induced Cellular Senescence

Subconfluent RPE cells grown on chamber slides were treated with 500  $\mu\text{M}$   $\text{H}_2\text{O}_2$  alone or 500  $\mu\text{M}$   $\text{H}_2\text{O}_2$  and 10  $\mu\text{g}/\text{mL}$  HN for 2 hours. The  $\text{H}_2\text{O}_2$  treatment was repeated the next day. The medium was replaced with fresh medium containing 10% FBS. It has been reported in ARPE-19 cells that serum starvation inhibits cell proliferation but is not associated with induction of a senescent phenotype, as the cells are small and most are SA- $\beta$ -Gal negative (quiescence phenotype). On the other hand, in the presence of serum, doxorubicin, a DNA-damaging agent, causes the senescent phenotype.<sup>39</sup> Cells were kept for 48 hours and medium was replaced every 24 hours. Humanin (10  $\mu\text{g}$ ) was present in one of the wells previously cotreated with  $\text{H}_2\text{O}_2$  and HN. A commercially available kit was used to detect SA- $\beta$ -Gal expression (Sigma-Aldrich Corp.). The RPE cells were stained with an X-gal-containing staining mixture for 8 hours at 37°C, and both blue-stained cells and total cells were

counted by microscopic inspection.<sup>6</sup> In addition to SA- $\beta$ -Gal staining, we also studied the expression of senescent marker p16<sup>INK4a</sup> by immunoblot analysis and *ApoJ* mRNA by real-time PCR.

### Transepithelial Resistance Measurements With CellZscope

The CellZscope (Nanoanalytics, Münster, Germany) measures the impedance of barrier-forming cell cultures grown on permeable membranes and provides the TER as output. Cells were seeded on cell culture inserts for 1 month in 1% FBS-containing medium. Both apical and basal cellular compartments were cotreated one time with various concentrations of HN (1–10  $\mu\text{g}/\text{mL}$ ) and 500  $\mu\text{M}$  tBH. CellZscope module-holding inserts remained in the incubator throughout the experiment to maintain optimum physiological conditions. Transepithelial resistance was measured automatically every 30 minutes for 95 hours.

### Statistics

Statistical analysis was performed by using ANOVA, followed by Tukey post-test using Graphpad InStat (version 3.05; GraphPad Software, San Diego, CA, USA). Data are presented as mean  $\pm$  SEM.  $P < 0.05$  was considered significant.

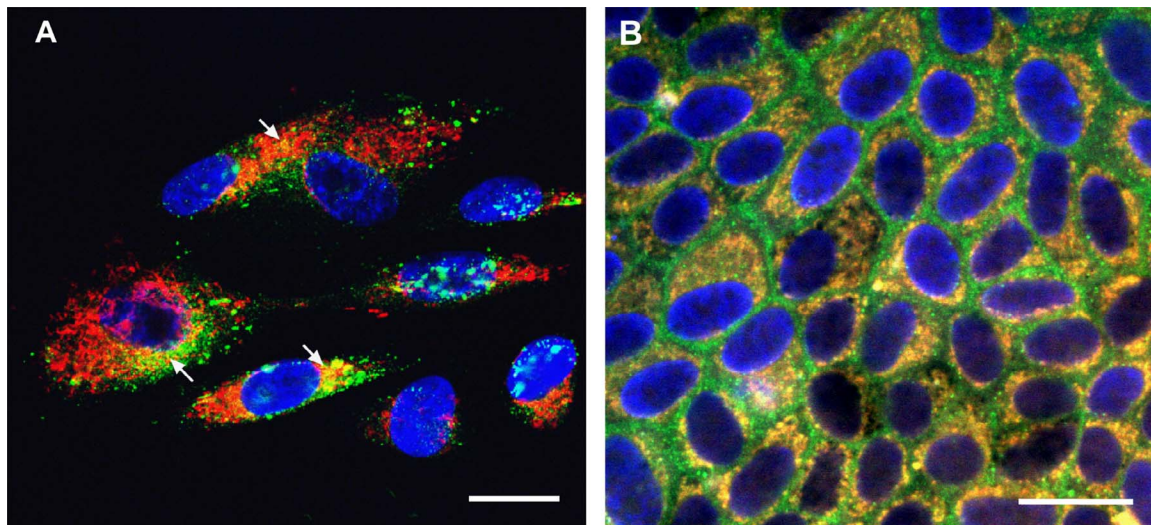


**FIGURE 2.** Humanin colocalized with mitochondria in RPE cells. Primary cultured nonpolarized RPE (A) and polarized RPE cells (B) were double-stained with HN and mitochondrial tracker. Nuclei were stained with DAPI (blue). Colocalization is visualized by yellow staining in the merged image for HN (green) and mitochondria (red) in RPE cells (arrows). The colocalization appeared to be more prominent in polarized RPE monolayer than nonpolarized RPE (B). Scale bar: 20  $\mu$ m.

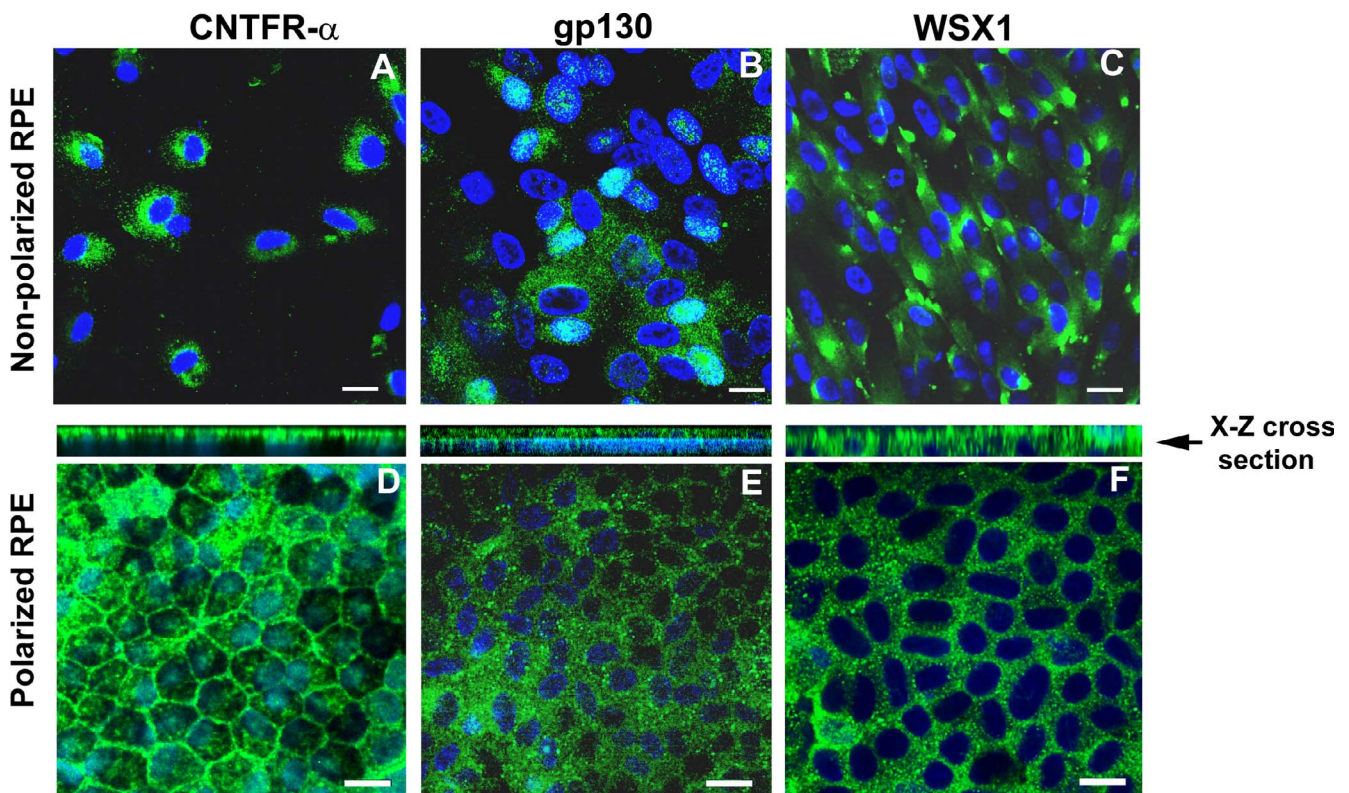


**FIGURE 3.** Nonpolarized RPE cells and polarized RPE monolayers expressed HN receptors. Expression of CNTFR $\alpha$ , gp130, and WSX1 in nonpolarized (A–C) and polarized RPE cells (D–F). Nuclear staining was performed with DAPI (blue). CNTFR $\alpha$  and WSX1 mostly localized in the cytoplasmic compartments, while gp130 showed nuclear as well as cytoplasmic localization. However, in polarized RPE monolayers, all the proteins were found predominately in the cytoplasm. The x-z cross-section stack image demonstrated that CNTFR $\alpha$  and gp130 are expressed on the apical side, while WSX1 is expressed in apical as well as basal domains. Scale bar: 20  $\mu$ m.

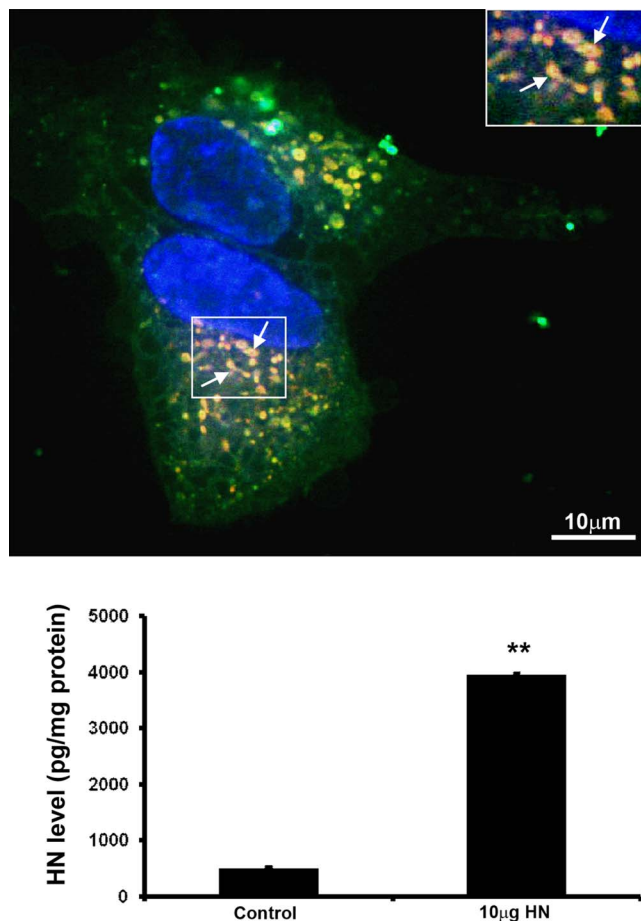


**FIGURE 4.** Uptake and translocation of FITC-labeled HN peptides in hRPE cells. Serum-starved nonpolarized RPE cells were incubated with 10 µg FITC-labeled HN for 2 hours. Uptake of labeled HN by RPE (upper panel). Fluorescent signal was evident in the cytosol and mitochondria (yellow merge). Arrow points to mitochondria colocalized with HN (inset). Nonpolarized RPE cellular HN levels were measured by ELISA after incubation with 10 µg HN for 24 hours. A significant 7.7-fold increase in HN levels was observed in RPE cells treated with HN, demonstrating uptake of HN by RPE cells (lower panel). \*\* $P < 0.001$ . Red: Mitotracker. Green: Humanin. Yellow: Merge. Scale bar: 10 µm.

## RESULTS

### Humanin Expression in Human RPE Cells, Its Subcellular Localization, and Characterization of Its Receptors

Polarized RPE monolayers mimic the native RPE monolayer, are resistant to cell death induced by oxidative stress, and have higher levels of certain cytoprotective growth factors than nonpolarized RPE.<sup>33–35</sup> In nonpolarized RPE cells, HN localized to the cytoplasmic compartments (Fig. 1A). A similar expression pattern was observed in polarized RPE cells (Fig. 1B), where the staining was found in both apical and basolateral domains (Fig. 1B). “No primary antibody” control is shown in Figure 1C. To study subcellular localization of HN, we costained RPE cells with Mitotracker Red and HN antibody. Humanin colocalized extensively with mitochondria in the cytoplasm in nonpolarized RPE cells but was also seen in the cytoplasm outside of mitochondria (Fig. 2A). To examine whether HN colocalization pattern is altered with differentiation, we double-stained polarized RPE monolayers with HN and Mitotracker Red. As

shown in Figure 2B, HN colocalized with mitochondria in RPE monolayer; however, the colocalization appeared to be even more pronounced in polarized than nonpolarized RPE cells. For further characterization of the HN transcript, we performed PCR with the following mitochondria-specific primer pairs (forward primer: AATCACTTGTTCCCTTAAATAGGGACC; reverse primer: GGGTCTTCTCGTCTTGCTGTG). Our PCR data showed that human RPE contained mitochondria-specific HN transcript (Supplementary Fig. S1).

We evaluated the expression of CNTFR $\alpha$ , WSX1, and gp130 in hRPE cells. All three receptors were expressed in both nonpolarized and polarized hRPE cells (Figs. 3A–F). CNTFR $\alpha$  and gp130 showed polarized localization, predominately localized to the apical domain, while WSX1 showed apical as well as basal localization (Figs. 3D–F). Since RPE cells expressed HN receptors, we measured HN secretion in the supernatants from both control and tBH-treated just confluent nonpolarized RPE cells ( $n = 3$ ). The mean ( $\pm$ SEM) concentration of HN in the supernatants was  $370.5 \pm 43.24$  pg/mL in control and  $525 \pm 86.63$  pg/mL in RPE cells treated with 150 µM tBH. Although there was a trend for an increase in HN levels in the supernatants of tBH-treated cells, it did not reach statistical significance. We also measured 24-hour HN secretion in the apical and basolateral media from polarized RPE monolayers. The mean ( $\pm$ SEM) concentration of HN in the apical and basolateral supernatants was  $936.6 \pm 45$  pg/mL and  $948.6 \pm 177$  pg/mL, respectively.

### Uptake of Exogenously Added Fluorescein-Labeled HN Peptide by RPE Cells and Colocalization With Mitochondria

Next, we investigated the uptake of exogenous HN by nonpolarized RPE cells and whether exogenous HN is taken up by mitochondria. The hRPE cells were incubated with 10 µg fluorescein-labeled HN peptide for 2 hours in serum-free medium. The HN peptide was predominantly taken up by RPE mitochondria (Fig. 4, inset), but was also found in cytoplasmic compartments (Fig. 4, upper panel). We further measured cellular HN levels in nonpolarized RPE cells treated with 10 µg HN for 24 hours. The levels of cellular HN were a significant 7.7-fold higher ( $P < 0.01$ ) in cells cotreated with exogenous HN over control cells (Fig. 4, lower panel), providing support for cellular uptake of exogenous HN by RPE cells.

### Humanin Protects RPE Cells From Oxidative Stress–Induced Cell Death: Polarized RPE Cells Are Highly Resistant to Oxidative Stress–Induced Cell Death

To study whether HN peptide offers protection to hRPE cells from oxidative stress, we coincubated just confluent nonpolarized hRPE cells with 150 µM tBH and 5 or 10 µg HN for 24 hours. We chose the above HN coincubation protocol from our initial studies of RPE cells with HN preincubation or coincubation and tBH treatment. There was no significant difference in the extent of cellular protection of RPE between preincubation and coincubation with HN (Supplementary Fig. S2). Our data revealed that HN protected hRPE cells effectively from cell death (Fig. 5A). We found a dose-dependent cell protection, and cell survival was highly significant ( $P < 0.01$ ) when compared with that of tBH-treated cells (Fig. 5B). The HN cotreatment also reduced mitochondrial superoxide production induced by tBH (Fig. 5C). In nonstressed RPE cells, Bax was found to be mostly localized in the cytoplasmic compartments (Fig. 5D). The tBH treatment resulted in extensive colocalization of Bax with the mitochondria marker,

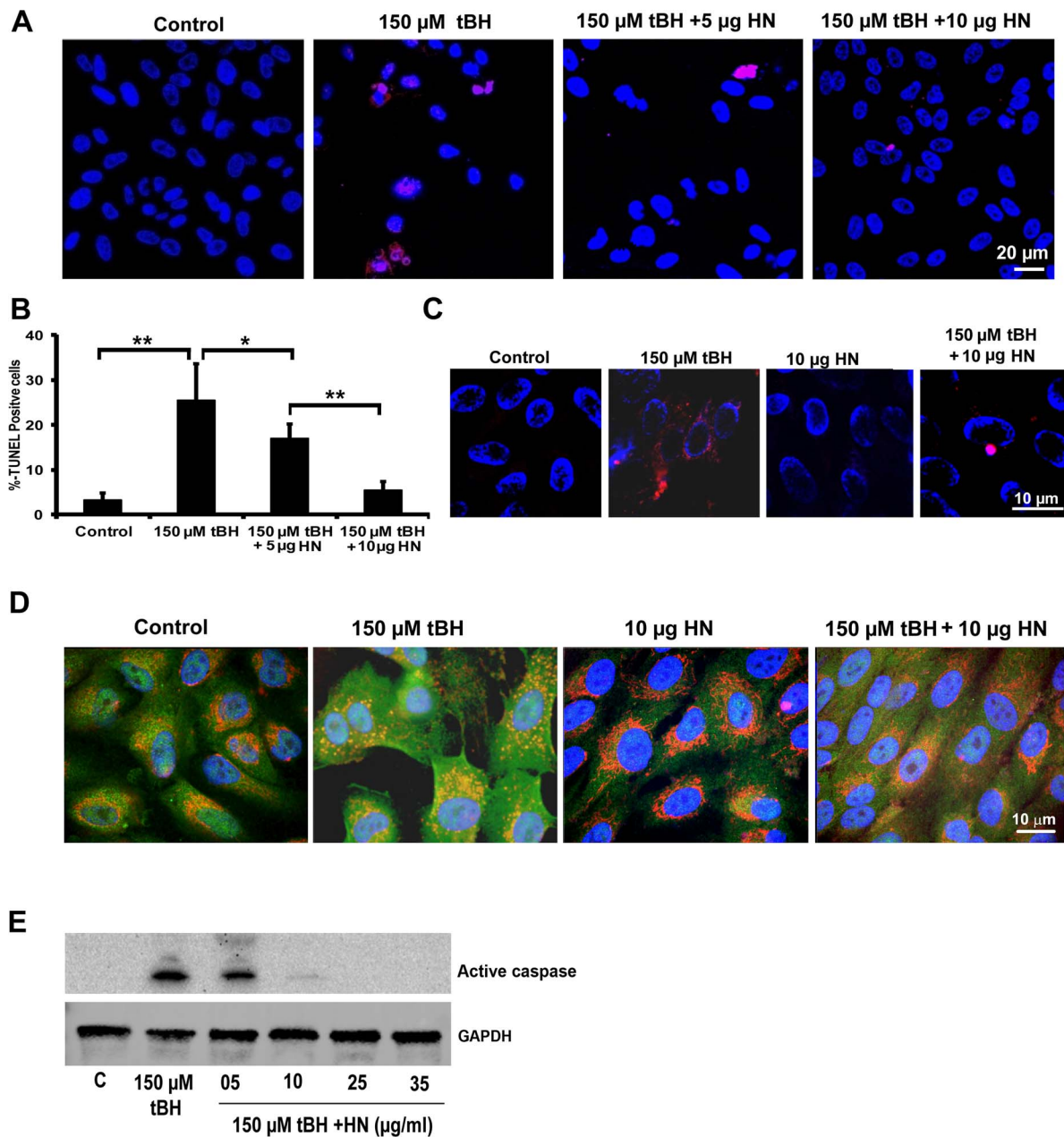


**FIGURE 5.** Exogenously added HN peptide protects nonpolarized RPE cells from cell death. (A) Human nonpolarized RPE cells were treated with single dose of 150  $\mu$ M tBH or 150  $\mu$ M tBH plus varying doses of HN (5, 10, 25, 35  $\mu$ g/mL) for 24 hours, and cell death was studied by TUNEL staining (red). Cell death was significantly higher in tBH-treated cells than in cells cotreated with HN and tBH. (B) Quantification of the TUNEL-positive cells. (C) Exogenously added HN inhibits mitochondrial ROS. The RPE cells were treated with 150  $\mu$ M tBH or 150  $\mu$ M tBH and varying doses of HN (10, 25, 35  $\mu$ g/mL) for 24 hours. The tBH treatment induced mitochondrial ROS (red) formation in RPE cells, which was inhibited by HN cotreatment. (D) Colocalization of Bax and mitochondria in RPE cells treated with and without tBH and HN. Primary cultured human RPE cells were double-stained with Bax (green) and Mitotracker (red). Nuclei were stained with DAPI (blue). Colocalization of Bax and mitochondria is visualized by yellow staining in the merged images. In untreated control cells, Bax is mostly localized in the cytoplasm, while oxidative stress translocated Bax to the mitochondria. Humanin cotreatment inhibited Bax mitochondrial translocation as evidenced by cytoplasmic staining of Bax. (E) Western blot shows activation of caspase-3 by tBH and inhibition of caspase-3 activation with varying doses of HN cotreatment. \* $P$  < 0.01, \*\* $P$  < 0.001.

indicating Bax translocation. Humanin cotreatment inhibited translocation of Bax to the mitochondria as demonstrated by cytosolic staining of Bax with much reduced mitochondrial colocalization (Fig. 5D). In addition, oxidative stress-induced activation of caspase-3 showed a dose-dependent decrease with HN coinubation and almost complete inhibition with higher HN doses (Fig. 5E).

Polarized RPE monolayers exhibit high TER and are highly resistant to oxidative stress-induced cell death, and only high

doses of oxidative stress can cause significant decrease in TER.<sup>35,40</sup> We treated polarized RPE cells with a single dose of 150  $\mu$ M tBH or 150  $\mu$ M tBH + 10  $\mu$ g HN applied to the apical and basolateral sides for 24 hours. Cell death was assessed by TUNEL staining. No significant alteration in TER was found in oxidative stress-induced RPE monolayers (control: 518  $\pm$  70  $\Omega$ ·cm<sup>2</sup> versus tBH-treated cells: 504  $\pm$  62  $\Omega$ ·cm<sup>2</sup>). Cell death was minimal in oxidative stress-induced cells under these experimental conditions (Figs. 6A, 6B). We hypothesized that

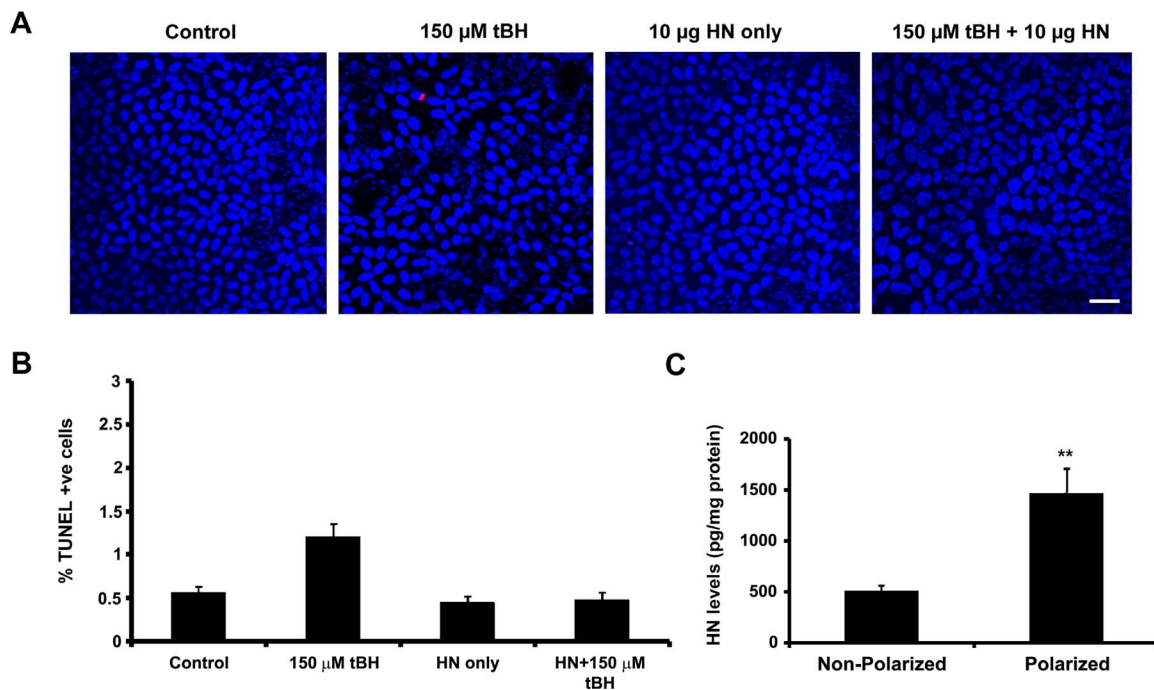


**FIGURE 6.** Higher cellular HN levels render polarized RPE monolayers more resistant to cell death. (A) Polarized RPE cells were treated with a single dose of 150  $\mu$ M tBH or 150  $\mu$ M tBH and 10  $\mu$ g HN applied to the apical and basolateral sides for 24 hours and cell death was assessed by TUNEL staining. Oxidant-induced cell death in polarized cells was considerably lower than that of nonpolarized cells (see Fig. 4) and HN decreased cell death. (B) Quantification of TUNEL-positive cells. (C) Cellular HN levels in nonpolarized and polarized RPE cells were measured in unstressed cells by ELISA analysis. Cellular HN level showed a 3-fold increase in polarized cells when compared with nonpolarized RPE cells. *Red*: TUNEL-positive cells. *Blue*: Nuclear marker (DAPI). Scale bar: 20  $\mu$ m. \*\* $P < 0.01$ .

increased resistance to oxidative stress could be related to higher cellular levels of HN, and as anticipated, the cellular levels of HN measured by ELISA showed a 3-fold increase in polarized RPE over nonpolarized RPE cells (Fig. 6C). When polarized cells were treated with a higher tBH dose (500  $\mu$ M) for 24 hours, we found 4% cell death, which decreased to 2% in HN-cotreated cells (Figs. 7A, 7B). No significant change in TER was noticed in RPE monolayers treated with 500  $\mu$ M tBH for 24 hours. However, over time, TER dropped significantly with the appearance of floating cells over the membrane. Figure 7C shows the time-dependent changes in TER in the presence of a constant dose of tBH (500  $\mu$ M) and varying doses of HN. Severe oxidative stress (500  $\mu$ M tBH) resulted in a significant ( $P < 0.001$  versus untreated controls) loss of TER (Fig. 7C). This resulted from significantly high percentage (77%) of cell death and subsequent disruption in the pattern and loss of tight junction protein ZO1<sup>35</sup> (Figs. 7D–H). Cotreatment with a single dose of HN in the dose range of 1 to 10  $\mu$ g maintained TER, which remained stable until 95 hours.

### Oxidative Stress Altered Mitochondrial Bioenergetics in RPE Cells, and HN Reestablished Mitochondrial Functions

We investigated the effects of oxidative stress and the role of HN in mitochondrial function in just confluent nonpolarized RPE cells. Oxygen consumption rate was determined in the presence of different inhibitors and uncoupling agents. The OCRs expressed as pmoles/minute/mg protein for all experimental groups were significantly different ( $P < 0.01$ ) from those of the untreated control cells (Figs. 8A–E). The basal respiration was significantly higher in controls and all HN-treated cells (Fig. 8A). Basal OCR was 3.5-fold lower in tBH-

treated cells than in control cells, and HN cotreatment showed a significant dose-dependent increase in basal OCR (Fig. 8A). To assess the effect of oxidative stress on mitochondrial bioenergetics, we treated RPE with 150  $\mu$ M tBH for 24 hours before the mitochondrial bioenergetic profile was assessed. Treatment with tBH significantly decreased basal respiration, ATP turnover, maximal OCR, mitochondrial reserve capacity, and proton leak over control cells (Figs. 8A–E). Humanin-cotreated cells exhibited a significantly ( $P < 0.01$  versus tBH-treated group) greater OCR owing to ATP synthase and increased mitochondrial oxygen reserve capacity (Figs. 8B, 8D).

### Increased Mitochondrial Biogenesis and Its Regulatory Molecules in HN-Treated RPE Cells

Because there was an increase in mitochondrial bioenergetics with HN treatment, we investigated whether HN cytoprotection is a result of increased mitochondrial biogenesis. There was a significant increase ( $P < 0.05$ ) in mtDNA copy number in just confluent nonpolarized RPE cells cotreated with HN plus tBH when compared to tBH-alone-treated cells (Fig. 9A). We also found approximately 50% increase in mtDNA copy number in control cells treated with HN compared to untreated cells but this did not reach statistical significance. We then counted the number of mitochondria per cell by TEM and showed a significant increase ( $P < 0.05$ ) in the mitochondria number in RPE cells treated with HN plus tBH over tBH alone (Figs. 9B, 9C). Because there was an increase in DNA copy number and mitochondria, we evaluated the protein level of mtTFA by Western blot, since this protein regulates mitochondrial transcription and genome copy number.<sup>41,42</sup> There was a significant upregulation of mtTFA in both control ( $P < 0.05$ ) and tBH-treated cells ( $P < 0.01$ ) when treated with

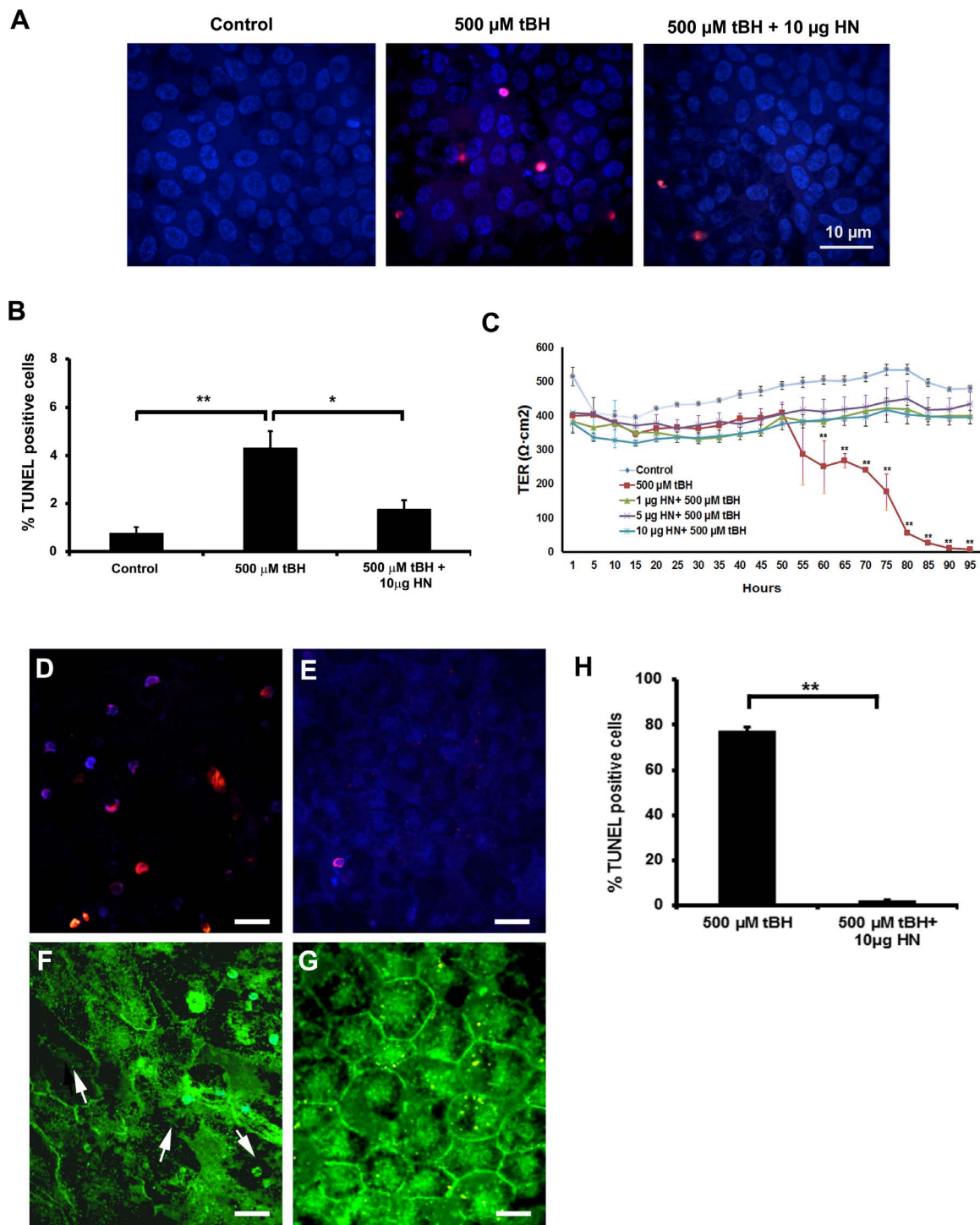


**FIGURE 7.** Polarized RPE monolayers more resistant to cell death; HN restored TER in oxidatively challenged polarized RPE cells. **(A)** Polarized RPE monolayers were treated with 500  $\mu\text{M}$  tBH or 500  $\mu\text{M}$  tBH and 10  $\mu\text{g}$  HN for 24 hours, and cell death was assessed by TUNEL staining. **(B)** Quantitation of TUNEL-positive cells. Increased cell death observed in tBH-treated cells, which was reduced in HN cotreated cells. **(C)** Polarized RPE monolayer was challenged with 500  $\mu\text{M}$  tBH or 500  $\mu\text{M}$  tBH plus varying doses (1, 5, 10  $\mu\text{g}/\text{mL}$ ) of HN, and TER was measured as a function of time. After 55 hours of tBH treatment, TER was significantly reduced and remained at the reduced level for the entire period of the experiment. Coincubation with HN maintained TER. The restoration of TER was similar with all doses tested. Polarized RPE cells were treated with 500  $\mu\text{M}$  tBH and 500  $\mu\text{M}$  tBH + 10  $\mu\text{g}$  HN for 95 hours. Cell death and tight junction protein ZO1 were examined by TUNEL staining and immunofluorescence staining, respectively. Significant cell death was found in monolayers treated with tBH alone, while HN coincubation protected RPE monolayer **(D, E)**. The tBH treatment resulted in severe breaks (*arrows*) in ZO1, and HN cotreatment prevented barrier breaks **(F, G)**. *Red*: TUNEL-positive cells. *Blue*: Nuclear marker (DAPI). *Green*: HN staining. Quantification of TUNEL-positive cells (shown in **[D, E]**) from three experiments **(H)**. Scale bar: 10  $\mu\text{m}$ . \* $P < 0.05$ , \*\* $P < 0.001$ .

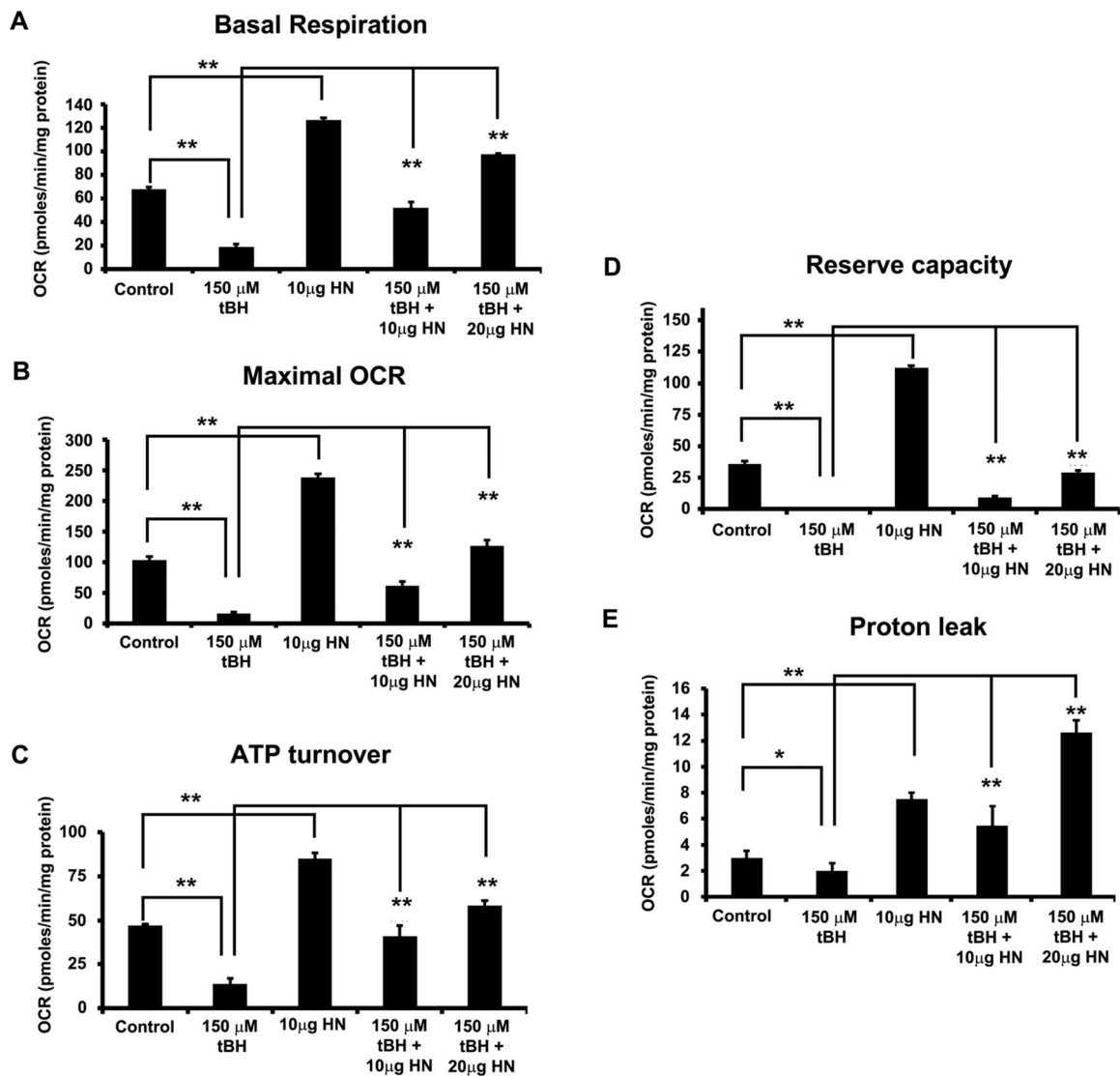


**FIGURE 8.** Humanin increased mitochondrial respiration rate in RPE cells. Real-time continuous measurement of mitochondrial respiration in RPE cells. Oxygen consumption rate was determined in nonpolarized RPE cells treated with 150  $\mu$ M tBH or 150  $\mu$ M tBH plus 10 or 20  $\mu$ g/mL HN or 10  $\mu$ g/mL HN only for 24 hours. Basal respiration (A), maximal OCR (B), ATP turnover (C), reserve capacity (D), and proton leak (E) were significantly reduced in tBH-treated cells versus control, whereas HN cotreatment increased all mitochondrial metabolic parameters studied when compared to tBH-treated group. \* $P < 0.01$ , \*\* $P < 0.01$ .

HN (Figs. 9D, 9E). Collectively, our data strongly support the contention that HN increases mitochondrial biogenesis.

### Protection of RPE by HN Is Partly Mediated by STAT3

Humanin exerts its protective function through different pathways, one of which is reported to be mediated through STAT3.<sup>28,43</sup> Humanin treatment increased phosphorylation of STAT3 in just confluent RPE cells at 2 hours, continuing until 24 hours (Fig. 10A). We wished to test whether a specific inhibitor of STAT3 would affect cell protection from tBH-induced oxidative injury. To achieve this, we treated confluent RPE cells for 24 hours with 150  $\mu$ M tBH or 150  $\mu$ M tBH + 10  $\mu$ g HN or 150  $\mu$ M tBH + 10  $\mu$ g HN along with 0.5  $\mu$ M STAT3 inhibitor. Cell death was studied by TUNEL staining. Treatment of RPE cells with tBH showed 20% cell death (Figs. 10B, 10C), which was blocked by HN coinubation. In the presence of STAT3 inhibitor, the percentage of cell death rebounded to 13%

(Figs. 10B, 10C). Treatment with tBH resulted in the activation of caspase-3 (Fig. 10D), while cotreatment with HN suppressed caspase-3 activation. Cotreatment with STAT3 inhibitor diminished the protective effect of HN significantly, as shown by increased caspase-3 activation, indicating a role for STAT3 in HN-mediated cell protection (Fig. 10E).

### Humanin Delayed Oxidative Stress-Induced Senescence in RPE Cells

Our recent work has reported that HN declines with age in mice and humans.<sup>44</sup> To test the hypothesis that HN inhibits cellular senescence, we used an oxidative stress-induced senescence model, where subconfluent hRPE cells were treated with 500  $\mu$ M H<sub>2</sub>O<sub>2</sub>. Oxidative stress treatment showed a significant ( $P < 0.01$  versus control cells) increase in senescence-associated  $\beta$ -Gal-positive cells (Fig. 11A). Treatment with 10  $\mu$ g HN for 48 hours had a significant ( $P < 0.01$  versus H<sub>2</sub>O<sub>2</sub>-treated cells) effect on the number of senescence-

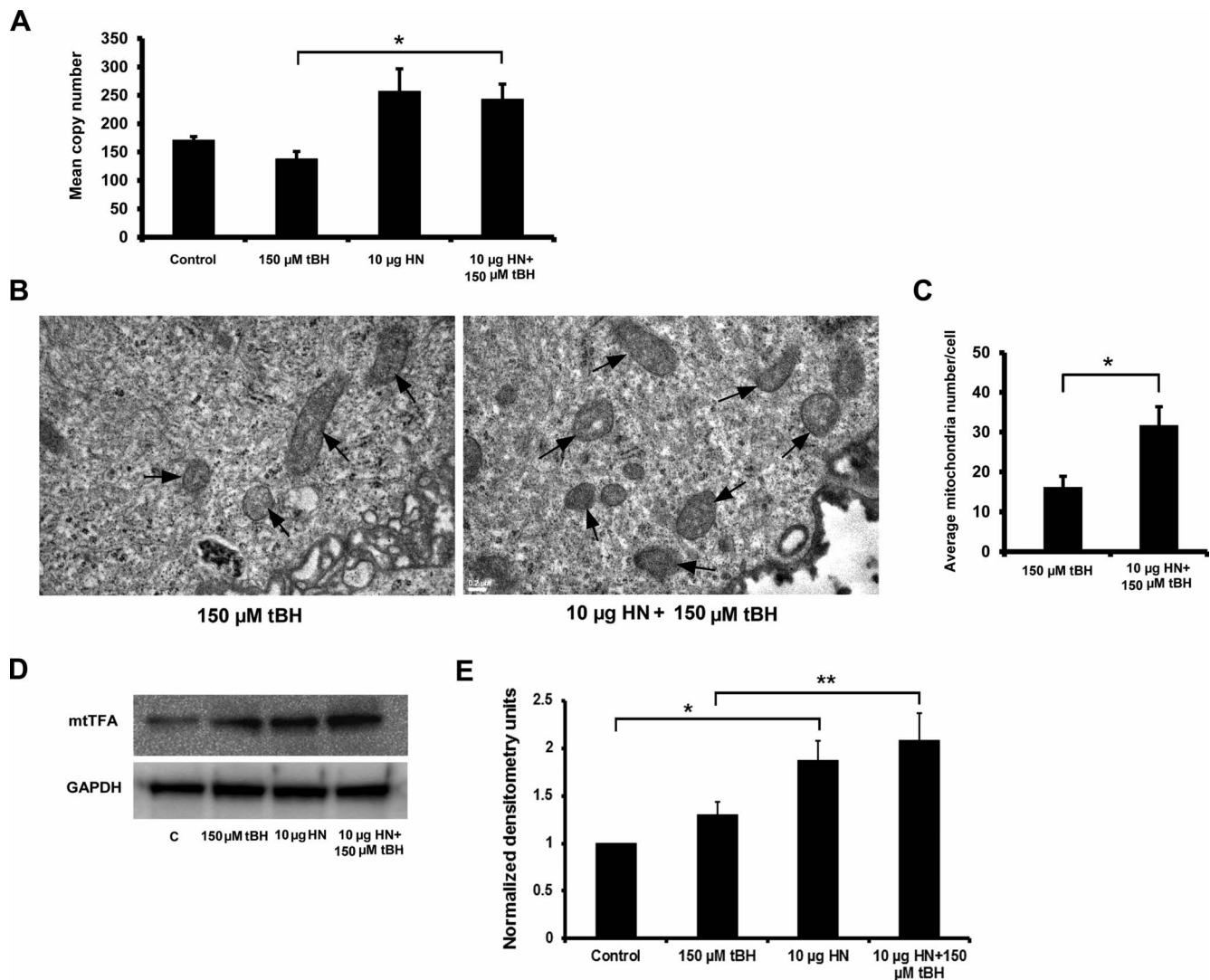


**FIGURE 9.** Humanin enhanced mitochondrial biogenesis in RPE cells. Nonpolarized RPE cells were treated with 150  $\mu$ M tBH or 10  $\mu$ g HN or 10  $\mu$ g HN + 150  $\mu$ M tBH for 24 hours and samples were analyzed for mitochondrial biogenesis by DNA copy number, TEM for mitochondrial number, and Western blot analysis for mtTFA. **(A)** The mtDNA copy numbers were determined by measuring the ratio of mtDNA to nuclear DNA (averaging the copy numbers of ND1/SLCO2B1 and ND5/SERPINA1) by real-time PCR. **(B, C)** Transmission electron microscopy was used to identify mitochondria (arrows) and quantitate mitochondrial number per cell in RPE cells treated with tBH and tBH plus HN. **(D, E)** Protein expression of mtTFA was measured by using Western blot analysis. The quantitative densitometry *bar graph* derived from three independent experiments showing significant upregulation of mtTFA with HN treatment. \* $P < 0.05$ , \*\* $P < 0.01$ . Scale bar: 0.2  $\mu$ m.

associated  $\beta$ -Gal-positive cells: a 50% decrease when compared to  $H_2O_2$  only-treated cells (Fig. 11B). Treatment with  $H_2O_2$  resulted in a significant 4-fold increase in *ApoJ* transcripts (a senescence marker), which was significantly ( $P < 0.01$ ) reduced with HN cotreatments (Fig. 11C). We further confirmed senescence by significant ( $P < 0.05$ ) upregulation of p16<sup>INK4a</sup>, while HN cotreatment decreased stress-induced senescence as seen by decreased expression of p16<sup>INK4a</sup> (Figs. 11D, 11E). However, we could not find any significant increase in senescence-associated  $\beta$ -Gal-positive cells or p16<sup>INK4a</sup> in RPE cells treated with 150  $\mu$ M tBH for 24 hours, the treatment condition used to study mitochondrial respiration (Supplementary Fig. S3).

## DISCUSSION

We provided evidence for the first time that HN and its receptors are expressed in RPE and that levels of cellular HN

are increased in polarized RPE monolayers, a finding that might explain their increased resistance to oxidative stress. Exogenous HN is taken up by RPE cells and much of the exogenous HN is colocalized with mitochondria. Our data provided strong evidence that HN protects RPE cells from oxidative stress-induced cell death via multiple mechanisms. The protection was achieved by the beneficial effect of HN on mitochondrial bioenergetics and biogenesis as evidenced by increased mitochondrial copy number and upregulation of mtTFA, a key protein involved in mitochondrial biogenesis. Additionally, HN activated STAT3 phosphorylation and inhibited caspase-3 activation. Furthermore, our study found for the first time that HN delays cellular senescence in vitro. Finally, exogenous HN maintained TER of polarized RPE monolayers from oxidative stress-induced cell injury, a finding that is highly relevant to HN's potential protective role in the normal RPE monolayer.

Since we were not able to study polarized RPE monolayers in the Seahorse XF Analyzer, we used the manufacturer's standard culture protocol as described in numerous publica-

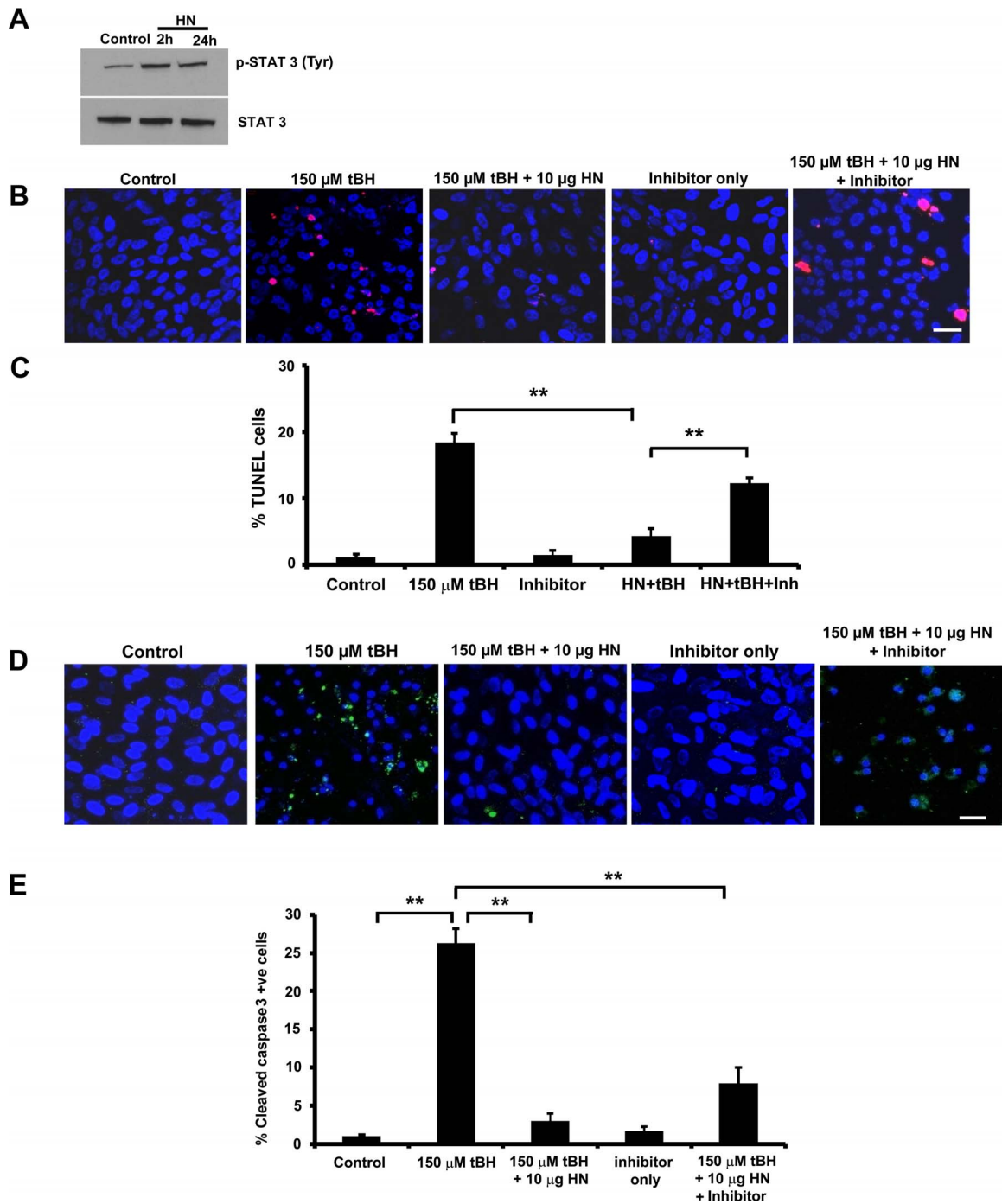


**FIGURE 10.** STAT3 inhibition augmented cell death and caspase-3 activation in RPE cells. (A) Nonpolarized RPE cells were treated with 10  $\mu$ g HN for 2 hours and 24 hours and cell lysate was subjected to immunoblot for phospho-STAT3 and total STAT3. (B) Nonpolarized RPE cells were treated with 150  $\mu$ M tBH or 150  $\mu$ M tBH plus 10  $\mu$ g/mL HN or 150  $\mu$ M tBH plus 10  $\mu$ g/mL HN plus 0.5  $\mu$ M STAT3 inhibitor or 0.5  $\mu$ M STAT3 inhibitor only for 24 hours. The TUNEL staining shows marked cell death in 150  $\mu$ M tBH-treated cells, which was significantly reduced with HN cotreatment. Inhibition of STAT3 with a STAT3 inhibitor increased cell death, suggesting a role for STAT3 in HN-mediated cell protection. (C) Quantification of TUNEL-positive cells. Data are presented as percentage of TUNEL-positive cells. (D) Confocal images showing increased active caspase-3 staining cells in tBH-treated cells. Caspase-3 staining was lower in HN cotreated cells, while STAT3 inhibition increased caspase-3 staining (E).  $**P < 0.01$ .

tions. At the same time, we believe use of RPE cells that are just confluent but not polarized is still highly relevant to late, atrophic AMD. It has been shown by Vogt et al.<sup>45</sup> that the normally polarized expression and localization of basolateral proteins, such as CD46 and MCT3, and an apical protein, ezrin, diminish with the progression of RPE alteration at a distance from the edge of the geographic atrophy lesion,

suggesting that early loss of polarity may be playing a role in progression of geographic atrophy (GA). Further, the authors suggest that RPE cells seen adjacent to the lesion are showing features of an RPE stress response.<sup>45</sup> Therefore, studying mitochondrial functions in the just confluent, but not polarized, RPE cells is of considerable significance in understanding the pathophysiology of GA.

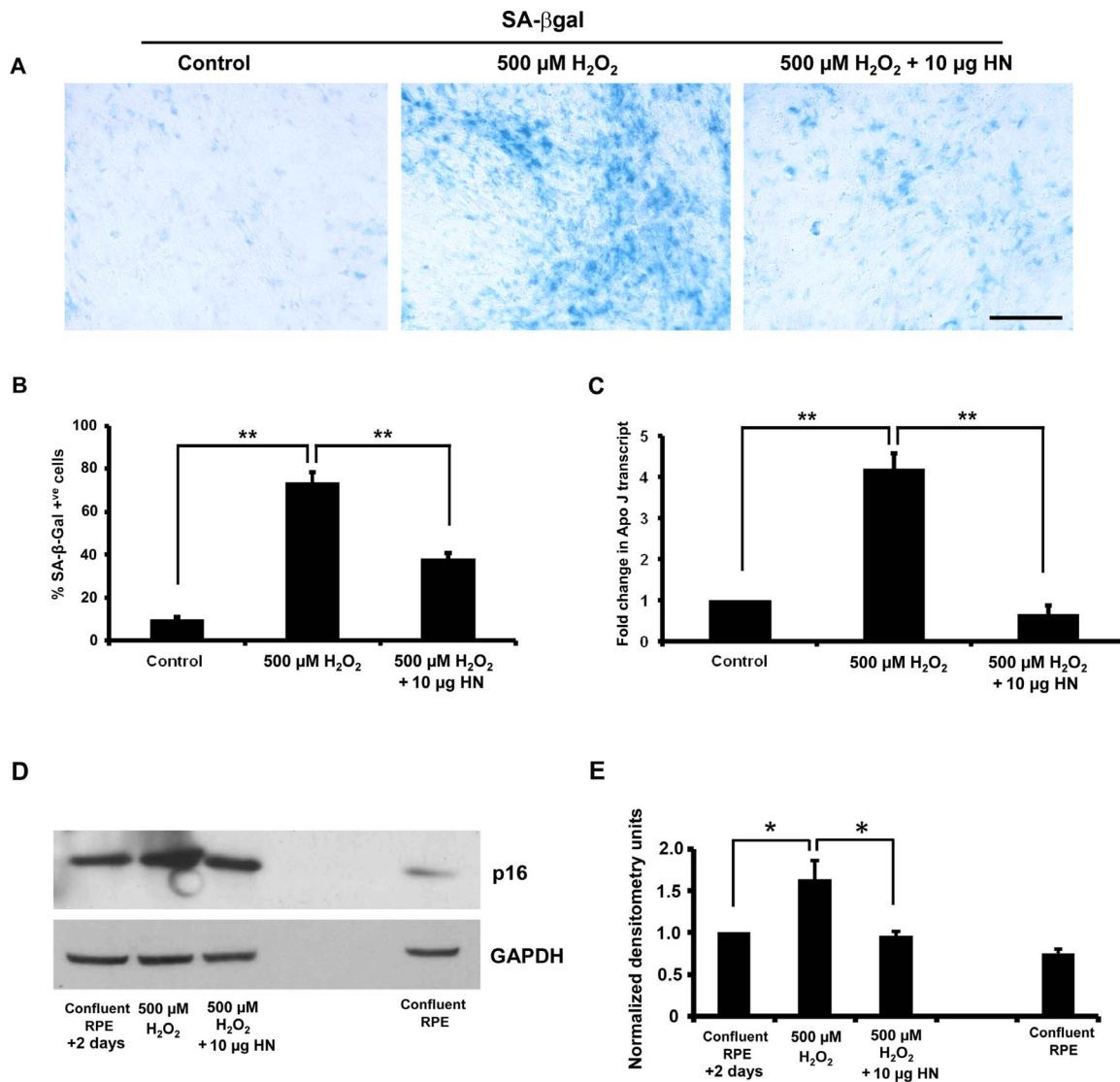


**FIGURE 11.** Humanin delays oxidative stress-induced senescence in RPE cells. The RPE cells were treated with 500  $\mu\text{M}$   $\text{H}_2\text{O}_2$  or 500  $\mu\text{M}$   $\text{H}_2\text{O}_2$  plus 10  $\mu\text{g}/\text{mL}$  HN and processed for SA- $\beta$ -Gal staining or p16<sup>INK4a</sup> immunoblot. Oxidative stress significantly increased the number of SA- $\beta$ -Gal-positive cells and RPE cell senescence was considerably lower with HN cotreatment (A, B). The  $\text{H}_2\text{O}_2$  treatment induced 75% cell senescence, whereas the HN cotreatment showed less than 30% cell senescence (B). (C) Gene expression of senescence marker gene *ApoJ* by real-time PCR (forward, 5'-AGAGTGTAAGCCCTG CCTGA-3'; reverse, 5'-CATCCAGAAGTAGAAGGGCG-3'). The expression of *ApoJ* was significantly higher in  $\text{H}_2\text{O}_2$ -treated cells than in control RPE cells. The increase in expression of *ApoJ* was significantly suppressed when cells were cocultured with HN. (D, E) Oxidative stress significantly increased expression of p16<sup>INK4a</sup>, while HN cotreatment restored p16<sup>INK4a</sup> expression to that of control cells. Expression of p16<sup>INK4a</sup> was considerably low in normal confluent RPE cells. \* $P < 0.05$ , \*\* $P < 0.01$ .

In the present study, cell death of RPE cells induced by the oxidant tBH was effectively blocked by HN cotreatment. The antiapoptotic effects of HN are well known in neuronal and other cell types.<sup>17,25,26,46-49</sup> Humanin has several modes of action, and its mechanism(s) appear(s) to be mediated via intracellular mitochondria-dependent pathways<sup>18,46,50</sup> and extracellular receptor complex-mediated pathways.<sup>23</sup> It has been suggested that exogenous HN can enter into certain cells.<sup>51</sup> Our laboratory has presented evidence that other peptides of similar length are taken up by RPE cells.<sup>52,53</sup> Our present data also showed that exogenous HN is rapidly taken up by RPE cells and localized within mitochondria, providing evidence for the participation of mitochondrial pathway in cellular protection. Further, we demonstrated the involvement of two pathways: one, mitochondria-dependent, via reactive oxygen species (ROS), resulting in subsequent changes in

mitochondrial bioenergetics and biogenesis; and the other, receptor-dependent via STAT3 phosphorylation.

While ROS may have important roles in cell function, high levels cause cell damage and death. Treatment of primary hRPE cells with tBH stimulates ROS formation and cell death, and a similar finding has been reported for ARPE-19 cells.<sup>54</sup> Supporting the ROS-induced translocation of Bax to the mitochondria, previous work has shown Bax mitochondrial translocation in cancer cells.<sup>55</sup> In fact, the formation of increased ROS could nullify or overcome normal antioxidant defenses and enhance opening of the mitochondrial permeability transition pore, membrane depolarization, ATP hydrolysis, and mitochondrial swelling, resulting in membrane break and release of prodeath proteins such as cytochrome c into the cytosol.<sup>16,56,57</sup> Despite strong evidence supporting mitochondria as a therapeutic target, very few available

peptides/drugs promote mitochondrial function. It should be noted that HN cotreatment significantly attenuated translocation of Bax to mitochondria, mitochondrial ROS formation, and cell death.

Humanin enhanced all measures of mitochondrial function in the XF study when added 24 hours before the measurements, strongly suggesting that the effect is due to enhanced mitochondrial biogenesis. Indeed, HN cotreatment significantly enhanced mitochondrial DNA copy number in tBH-treated cells and increased mitochondrial number. These results were strongly supported by the upregulation of mtTFA by HN in both control and tBH-treated cells. Mitochondrial TFA binds mitochondrial DNA and regulates mitochondrial transcription initiation, mtDNA copy number, packaging of mitochondrial DNA, and mitochondrial biogenesis.<sup>41,42,58-61</sup> Thus, HN enhances RPE protection from oxidative stress via increased mitochondrial biogenesis and bioenergetics and by inhibiting the translocation of Bax from cytosol to mitochondria and preventing cytochrome c release.<sup>14</sup> Effects of HN and its analogues on mitochondrial function have been described for human aortic endothelial cells, cardiac myoblasts, human lymphocytes, muscular TE671 cells, and neural SKN-MC cells.<sup>16,18,62</sup> However, this study is the first to demonstrate these effects may be manifested through improved mitochondrial bioenergetics and biogenesis. As alluded to earlier, we attempted from the beginning to study mitochondrial bioenergetics in both nonpolarized and polarized monolayers, and consulted with scientists and technical representatives from Seahorse; however, we could not identify any commercially available inserts for studying polarized monolayers in the Seahorse instrument. We attempted growth of polarized RPE in XF custom 96-well plates but careful evaluation of the cultures revealed irregular and inconsistent differentiation and formation of multilayers. We still believe it will be important to develop new techniques to study mitochondrial function in polarized RPE monolayers, using Seahorse instrument, and this will be a future priority.

Humanin may also be acting through activation of HN receptors that are expressed on RPE cells. The source of exogenous HN could be from the RPE cells themselves. Since HN has been reported to be a secreted protein in certain neuronal cells,<sup>9</sup> we hypothesized that RPE cells could also secrete HN. Herein we described the release of HN by RPE cells into cell supernatants in both control and tBH-treated cells. Polarized RPE cells secrete HN from both apical and basolateral sides almost in equal proportions. It is likely that there are other cell types in the retina that express HN and probably secrete HN. Animal studies will be able to address differential roles of local versus serum-derived HN. Given the above finding, we explored extracellular cytoprotective pathways of HN. The cytoprotective effect of HN has been reported to be mediated by phosphorylation of STAT3 through a heterotrimeric cell-surface cytokine receptor complex.<sup>25,26,28,48</sup> We showed significant activation and phosphorylation of STAT3 in RPE cells after 2-hour treatment with HN, and this effect persisted to 24 hours. A protective role of STAT3 has been demonstrated in ischemia and reperfusion injury, and deletion of STAT3 shows enhanced susceptibility to injury.<sup>63</sup> Consistent with these findings, STAT3 inhibition enhanced oxidative stress-induced activation of caspase-3 and cell death in human RPE cells; however, while the effect was significant, it did not account for all instances of cell death caused by the oxidant. Therefore, it has to be reasoned that the receptor-mediated effects of HN peptide only partially contributed to the prevention of cell death. Taken together, these results indicate that ROS-

mediated signaling mechanism is also important in the protection of RPE cells.

One remarkable impact of oxidative stress is the initiation of cellular senescence, and premature senescence has been suggested as a potentially important pathophysiological mediator of RPE cell atrophy in GA.<sup>8,64</sup> Senescence-associated  $\beta$ -Gal staining has been observed in RPE cells adjacent to cuticular drusen of aged monkeys.<sup>65</sup> The expression of several genes that code for proteins involved in maintaining cell structure is altered in senescent RPE cells; and altered gene expression could also impact RPE barrier functions.<sup>66</sup> We found that HN treatment significantly reduced senescence-associated  $\beta$ -Gal-positive cells, *ApoJ* transcripts, and p16<sup>INK4a</sup> expression. A positive correlation between HN levels and longevity has been demonstrated in different mouse models.<sup>44</sup> Further, circulating levels of HN decline with age in mice and humans, indicating age-dependent regulation of its expression.<sup>67</sup> However, whether the level of HN decreases in aged RPE is not clear at this time. Our study provided evidence that HN can correct oxidative stress-induced alterations in TER to those of control RPE monolayers, thereby improving membrane integrity. Therefore, a promising therapeutic approach to preventing RPE senescence may be to increase cellular HN levels.

To summarize, HN protection of RPE cells from oxidative stress is mediated via dual mechanisms: by enhancing mitochondrial function and biogenesis and via activation of STAT3. Further, HN inhibited oxidative stress-induced cell senescence and maintained TER in human RPE monolayers. Given the multipotent effects of HN in protecting against inflammation, mitochondrial oxidative stress,  $\beta$ -amyloid toxicity, senescence, and neurotoxicity, HN and its analogues could prove to be a valuable therapeutic approach for AMD, especially GA.

### Acknowledgments

We thank Ernesto Barron for assistance with figures, and Douglas Hauser and Anthony Rodriguez for technical assistance with electron microscopy.

Supported in part by Grants EY01545 (DRH) and by Core Grant EY03040, the Arnold and Mabel Beckman Foundation (DRH), 1R01AG034430 (PC), 1R01GM090311 (PC), 1R01ES020812 (PC), 1P01AG034906 (PC), a Glen Foundation Award (PC), and an unrestricted grant to the Department of Ophthalmology from Research to Prevent Blindness, Inc.

Disclosure: **P.G. Sreekumar**, None; **K. Ishikawa**, None; **C. Spee**, None; **H.H. Mehta**, None; **J. Wan**, None; **K. Yen**, None; **P. Cohen**, CohBar, Inc. (I, C); **R. Kannan**, None; **D.R. Hinton**, None

### References

1. Ambati J, Ambati BK, Yoo SH, Ianchulev S, Adamis AP. Age-related macular degeneration: etiology, pathogenesis, and therapeutic strategies. *Surv Ophthalmol*. 2003;48:257-293.
2. de Jong PT. Age-related macular degeneration. *N Engl J Med*. 2006;355:1474-1485.
3. Klein R, Klein BE, Tomany SC, Meuer SM, Huang GH. Ten-year incidence and progression of age-related maculopathy: The Beaver Dam eye study. *Ophthalmology*. 2002;109:1767-1779.
4. Ding X, Patel M, Chan CC. Molecular pathology of age-related macular degeneration. *Prog Retin Eye Res*. 2009;28:1-18.
5. Matsunaga H, Handa JT, Gelfman CM, Hjelmeland LM. The mRNA phenotype of a human RPE cell line at replicative senescence. *Mol Vis*. 1999;5:39.

6. Zhu D, Wu J, Spee C, Ryan SJ, Hinton DR. BMP4 mediates oxidative stress-induced retinal pigment epithelial cell senescence and is overexpressed in age-related macular degeneration. *J Biol Chem*. 2009;284:9529-9539.
7. Rodier F, Campisi J. Four faces of cellular senescence. *J Cell Biol*. 2011;192:547-556.
8. Kozłowski MR. RPE cell senescence: a key contributor to age-related macular degeneration. *Med Hypotheses*. 2012;78:505-510.
9. Hashimoto Y, Niikura T, Tajima H, et al. A rescue factor abolishing neuronal cell death by a wide spectrum of familial Alzheimer's disease genes and Abeta. *Proc Natl Acad Sci U S A*. 2001;98:6336-6341.
10. Lee C, Yen K, Cohen P. Humanin: a harbinger of mitochondrial-derived peptides? *Trends Endocrinol Metab*. 2013;24:222-228.
11. Yen K, Lee C, Mehta H, Cohen P. The emerging role of the mitochondrial-derived peptide humanin in stress resistance. *J Mol Endocrinol*. 2013;50:R11-R19.
12. Tajima H, Niikura T, Hashimoto Y, et al. Evidence for in vivo production of Humanin peptide, a neuroprotective factor against Alzheimer's disease-related insults. *Neurosci Lett*. 2002;324:227-231.
13. Bodzioch M, Lapicka-Bodzioch K, Zapala B, Kamysz W, Kiec-Wilk B, Dembinska-Kiec A. Evidence for potential functionality of nuclearly-encoded humanin isoforms. *Genomics*. 2009;94:247-256.
14. Guo B, Zhai D, Cabezas E, et al. Humanin peptide suppresses apoptosis by interfering with Bax activation. *Nature*. 2003;423:456-461.
15. Paharkova V, Alvarez G, Nakamura H, Cohen P, Lee KW. Rat Humanin is encoded and translated in mitochondria and is localized to the mitochondrial compartment where it regulates ROS production. *Mol Cell Endocrinol*. 2015;413:96-100.
16. Klein LE, Cui L, Gong Z, Su K, Muzumdar R. A humanin analog decreases oxidative stress and preserves mitochondrial integrity in cardiac myoblasts. *Biochem Biophys Res Commun*. 2013;440:197-203.
17. Kariya S, Takahashi N, Ooba N, Kawahara M, Nakayama H, Ueno S. Humanin inhibits cell death of serum-deprived PC12h cells. *Neuroreport*. 2002;13:903-907.
18. Bachar AR, Scheffer L, Schroeder AS, et al. Humanin is expressed in human vascular walls and has a cytoprotective effect against oxidized LDL-induced oxidative stress. *Cardiovasc Res*. 2010;88:360-366.
19. Park TY, Kim SH, Shin YC, et al. Amelioration of neurodegenerative diseases by cell death-induced cytoplasmic delivery of humanin. *J Control Release*. 2013;166:307-315.
20. Kin T, Sugie K, Hirano M, Goto Y, Nishino I, Ueno S. Humanin expression in skeletal muscles of patients with chronic progressive external ophthalmoplegia. *J Hum Genet*. 2006;51:555-558.
21. Wang D, Li H, Yuan H, et al. Humanin delays apoptosis in K562 cells by downregulation of P38 MAP kinase. *Apoptosis*. 2005;10:963-971.
22. Chin YP, Keni J, Wan J, et al. Pharmacokinetics and tissue distribution of humanin and its analogues in male rodents. *Endocrinology*. 2013;154:3739-3744.
23. Matsuoka M, Hashimoto Y. Humanin and the receptors for humanin. *Mol Neurobiol*. 2010;41:22-28.
24. Ikonen M, Liu B, Hashimoto Y, et al. Interaction between the Alzheimer's survival peptide humanin and insulin-like growth factor-binding protein 3 regulates cell survival and apoptosis. *Proc Natl Acad Sci U S A*. 2003;100:13042-13047.
25. Hashimoto Y, Kurita M, Aiso S, Nishimoto I, Matsuoka M. Humanin inhibits neuronal cell death by interacting with a cytokine receptor complex or complexes involving CNTF receptor alpha/WSX-1/gp130. *Mol Biol Cell*. 2009;20:2864-2873.
26. Hashimoto Y, Kurita M, Matsuoka M. Identification of soluble WSX-1 not as a dominant-negative but as an alternative functional subunit of a receptor for an anti-Alzheimer's disease rescue factor Humanin. *Biochem Biophys Res Commun*. 2009;389:95-99.
27. Chiba T, Yamada M, Hashimoto Y, et al. Development of a femtomolar-acting humanin derivative named colivelin by attaching activity-dependent neurotrophic factor to its N terminus: characterization of colivelin-mediated neuroprotection against Alzheimer's disease-relevant insults in vitro and in vivo. *J Neurosci*. 2005;25:10252-10261.
28. Hashimoto Y, Suzuki H, Aiso S, Niikura T, Nishimoto I, Matsuoka M. Involvement of tyrosine kinases and STAT3 in Humanin-mediated neuroprotection. *Life Sci*. 2005;77:3092-3104.
29. Luciano F, Zhai D, Zhu X, et al. Cytoprotective peptide humanin binds and inhibits proapoptotic Bcl-2/Bax family protein BimEL. *J Biol Chem*. 2005;280:15825-15835.
30. Zhai D, Luciano F, Zhu X, Guo B, Satterthwait AC, Reed JC. Humanin binds and nullifies Bid activity by blocking its activation of Bax and Bak. *J Biol Chem*. 2005;280:15815-15824.
31. Ohno-Matsui K. Parallel findings in age-related macular degeneration and Alzheimer's disease. *Prog Retin Eye Res*. 2011;30:217-238.
32. Sreekumar PG, Kannan R, Yaung J, Spee CK, Ryan SJ, Hinton DR. Protection from oxidative stress by methionine sulfoxide reductases in RPE cells. *Biochem Biophys Res Commun*. 2005;334:245-253.
33. Sonoda S, Spee C, Barron E, Ryan SJ, Kannan R, Hinton DR. A protocol for the culture and differentiation of highly polarized human retinal pigment epithelial cells. *Nat Protoc*. 2009;4:662-6673.
34. Sonoda S, Sreekumar PG, Kase S, et al. Attainment of polarity promotes growth factor secretion by retinal pigment epithelial cells: relevance to age-related macular degeneration. *Aging (Albany NY)*. 2009;2:28-42.
35. Sreekumar PG, Kannan R, Kitamura M, et al.  $\alpha$ B crystallin is apically secreted within exosomes by polarized human retinal pigment epithelium and provides neuroprotection to adjacent cells. *PLoS One*. 2010;5:e12578.
36. Dranka BP, Hill BG, Darley-Usmar VM. Mitochondrial reserve capacity in endothelial cells: the impact of nitric oxide and reactive oxygen species. *Free Radic Biol Med*. 2010;48:905-914.
37. Mitchell T, Johnson MS, Ouyang X, et al. Dysfunctional mitochondrial bioenergetics and oxidative stress in Akita(+/-Ins2)-derived  $\beta$ -cells. *Am J Physiol Endocrinol Metab*. 2013;305:E585-E599.
38. Yu Y, Liu H, Ikeda Y, et al. Hepatocyte-like cells differentiated from human induced pluripotent stem cells: relevance to cellular therapies. *Stem Cell Res*. 2012;9:196-207.
39. Demidenko ZN, Blagosklonny MV. Growth stimulation leads to cellular senescence when the cell cycle is blocked. *Cell Cycle*. 2008;7:3355-3361.
40. Zhu D, Sreekumar PG, Hinton DR, Kannan R. Expression and regulation of enzymes in the ceramide metabolic pathway in human retinal pigment epithelial cells and their relevance to retinal degeneration. *Vision Res*. 2010;50:643-651.
41. Campbell CT, Kolesar JE, Kaufman BA. Mitochondrial transcription factor A regulates mitochondrial transcription initiation, DNA packaging, and genome copy number. *Biochim Biophys Acta*. 2012;1819:921-929.
42. Lee CH, Wu SB, Hong CH, et al. Aberrant cell proliferation by enhanced mitochondrial biogenesis via mtTFA in arsenical skin cancers. *Am J Pathol*. 2011;178:2066-2076.

43. Hoang PT, Park P, Cobb LJ, et al. The neurosurvival factor Humanin inhibits beta-cell apoptosis via signal transducer and activator of transcription 3 activation and delays and ameliorates diabetes in nonobese diabetic mice. *Metabolism*. 2010;59:343-349.
44. Lee C, Wan J, Miyazaki B, et al. IGF-I regulates the age-dependent signaling peptide humanin. *Aging Cell*. 2014;13:958-961.
45. Vogt SD, Curcio CA, Wang L, et al. Retinal pigment epithelial expression of complement regulator CD46 is altered early in the course of geographic atrophy. *Exp Eye Res*. 2011;93:413-423.
46. Muzumdar RH, Huffman DM, Calvert JW, et al. Acute humanin therapy attenuates myocardial ischemia and reperfusion injury in mice. *Arterioscler Thromb Vasc Biol*. 2010;30:1940-1948.
47. Zacharias DG, Kim SG, Massat AE, et al. Humanin, a cytoprotective peptide, is expressed in carotid atherosclerotic [corrected] plaques in humans. *PLoS One*. 2012;7:e31065.
48. Jia Y, Lue YH, Swerdloff R, et al. The cytoprotective peptide humanin is induced and neutralizes Bax after pro-apoptotic stress in the rat testis. *Andrology*. 2013;1:651-659.
49. Eriksson E, Wickström M, Perup LS, et al. Protective role of humanin on bortezomib-induced bone growth impairment in anticancer treatment. *J Natl Cancer Inst*. 2014;106:djt459.
50. Jin H, Liu T, Wang WX, et al. Protective effects of [Gly14]-Humanin on beta-amyloid-induced PC12 cell death by preventing mitochondrial dysfunction. *Neurochem Int*. 2010;56:417-423.
51. Kariya S, Hirano M, Furiya Y, Ueno S. Effect of humanin on ATP production: therapeutic candidate for mitochondrial disorders. *Ann. Neurol*. 2004;56(S8):65.
52. Sreekumar PG, Chothe P, Sharma KK, et al. Antiapoptotic properties of  $\alpha$ -crystallin-derived peptide chaperones and characterization of their uptake transporters in human RPE cells. *Invest Ophthalmol Vis Sci*. 2013;54:2787-2798.
53. Wang W, Sreekumar PG, Valluripalli V, et al. Protein polymer nanoparticles engineered as chaperones protect against apoptosis in human retinal pigment epithelial cells. *J Control Release*. 2014;191:4-14.
54. Garg TK, Chang JY. Oxidative stress causes ERK phosphorylation and cell death in cultured retinal pigment epithelium: prevention of cell death by AG126 and 15-deoxy-delta 12, 14-PGJ2. *BMC Ophthalmol*. 2003;3:5.
55. Byun JY, Kim MJ, Eum DY, et al. Reactive oxygen species-dependent activation of Bax and poly(ADP-ribose) polymerase-1 is required for mitochondrial cell death induced by triterpenoid pristimerin in human cervical cancer cells. *Mol Pharmacol*. 2009;76:734-744.
56. Ong SB, Gustafsson AB. New roles for mitochondria in cell death in the reperfused myocardium. *Cardiovasc Res*. 2012;94:190-196.
57. Kubli DA, Gustafsson AB. Mitochondria and mitophagy: the yin and yang of cell death control. *Circ Res*. 2012;111:1208-1221.
58. Ikeda M, Ide T, Fujino T, et al. Overexpression of TFAM or twinkle increases mtDNA copy number and facilitates cardioprotection associated with limited mitochondrial oxidative stress. *PLoS One*. 2015;10:e0119687.
59. Yu J, Wang Q, Chen N, et al. Mitochondrial transcription factor A regulated ionizing radiation-induced mitochondrial biogenesis in human lung adenocarcinoma A549 cells. *J Radiat Res*. 2013;54:998-1004.
60. Quiñones-Lombrana A, Blanco JG. Chromosome 21-derived hsa-miR-155-5p regulates mitochondrial biogenesis by targeting Mitochondrial Transcription Factor A (TFAM). *Biochim Biophys Acta*. 2015;1852:1420-1427.
61. Bonawitz ND, Clayton DA, Shadel GS. Initiation and beyond: multiple functions of the human mitochondrial transcription machinery. *Mol Cell*. 2006;24:813-825.
62. Kariya S, Hirano M, Furiya Y, Ueno S. Effect of humanin on decreased ATP levels of human lymphocytes harboring A3243G mutant mitochondrial DNA. *Neuropeptides*. 2005;39:97-101.
63. Hilfiker-Kleiner D, Hilfiker A, Fuchs M, et al. Signal transducer and activator of transcription 3 is required for myocardial capillary growth, control of interstitial matrix deposition, and heart protection from ischemic injury. *Circ Res*. 2004;95:187-195.
64. Naylor RM, Baker DJ, van Deursen JM. Senescent cells: a novel therapeutic target for aging and age-related diseases. *Clin Pharmacol Ther*. 2013;93:105-116.
65. Matsunaga H, Handa JT, Aotaki-Keen A, Sherwood SW, West MD, Hjelmeland LM. Beta-galactosidase histochemistry and telomere loss in senescent retinal pigment epithelial cells. *Invest Ophthalmol Vis Sci*. 1999;40:197-202.
66. Shelton DN, Chang E, Whittier PS, Choi D, Funk WD. Microarray analysis of replicative senescence. *Curr Biol*. 1999;9:939-945.
67. Muzumdar RH, Huffman DM, Atzmon G, et al. Humanin: a novel central regulator of peripheral insulin action. *PLoS One*. 2009;4:e6334.